Interpretation of cirrus cloud polarization measurements from radiative transfer theory

K. N. Liou and Y. Takano

Department of Atmospheric Sciences, University of California, Los Angeles, California, USA

Received 20 December 2001; revised 19 February 2002; accepted 22 February 2002; published 10 May 2002.

[1] A theoretical framework has been developed for the computation of polarized radiative transfer involving ice crystal clouds to interpret the polarization pattern observed from space. Based on the limited available observations in near infrared window wavelengths, we demonstrate that the reflected linear or full polarization from sunlight can be employed to discriminate between spherical water droplets (water clouds) and nonspherical ice crystals (ice clouds) in the direction of rainbow angles, about 140° from the sun. In the case of ice clouds, we show that information regarding the ice crystal shape and orientation can be inferred from reflected polarization patterns based on a comprehensive theoretical interpretation. *INDEX TERMS:* 0320 Atmospheric Composition and Structure: Cloud physics and chemistry; 3359 Meteorology and Atmospheric Dynamics: Radiative processes; 3360 Meteorology and Atmospheric Dynamics: Remote sensing

1. Introduction

[2] Recent observations based on aircraft optical probes and replicator techniques for midlatitude, tropical, and contrail cirrus reveal that these clouds are largely composed of solid and hollow columns, plates, bullet rosettes, aggregates, and ice crystals with irregular surfaces. The size of these ice particles ranges from a few micrometers to about 1000 μm. Further, the fact that numerous halos and arcs have been observed demonstrates that a specific alignment of ice particles (i.e., horizontal) must exist in some cirrus. The horizontal orientation of ice particles in cirrus clouds has also been documented by numerous lidar measurements based on the depolarization technique in the backscattering direction. Horizontal orientation occurs when the ice particles have relatively large sizes and defined shapes, such as columns and plates. If the ice crystals are irregular, such as aggregates, horizontal alignment is unlikely to occur, as in the case for smaller ice crystals, which tend to be randomly oriented in space. However, it has been noted that ice particle alignment is closely modulated by the electric fields in clouds.

[3] Measurements of the polarization of sunlight reflected from planetary atmospheres have been used extensively for the exploration of composition information, beginning with the pioneering work done on Venus by the French astronomer *Lyot* [1929]. *Hansen and Hovenier* [1974] have performed an extensive investigation of the particle shape, size, and refractive index of the Venus cloud deck by comparing the observed linear polarization with comprehensive multiple scattering computations, including Lorenz-Mie spherical particles and Rayleigh molecules. The intriguing result from this study was the conclusion that the Venus cloud layer was composed of micron-sized spherical particles with a refractive index of about 1.44 at the 0.55 μm wavelength. *Takano and Liou* [1989] and *Liou and Takano* [1994] have used the light scattering results for randomly oriented hexagonal plates and columns and irregular ice particles to interpret the measured linear polarization of sunlight reflected from optically thick cirrus clouds that was reported by *Coffeen* [1979]. *Takano and Liou* [1993] have further presented the theoretical formulation and numerical calculations involving the transfer of polarized thermal infrared radiation emitted from the earth and clouds, specifically applied to horizontally oriented ice particles. More recently, measurements of the polarization of sunlight reflected from cirrus clouds have been reported by *Chepfer et al.* [1999a, 1999b] using a polarimeter, referred to as POLDER [Polarization and Directionality of the Earth's Reflectances].

[4] In this paper, we present a theoretical basis that is applicable to the computation of both solar and thermal radiative transfer including polarization for randomly and horizontally oriented ice crystals. Interpretation of polarization measurements involving cirrus clouds is subsequently carried out and we demonstrate that polarization of the scattered sunlight can be used to differentiate between spherical water droplets and nonspherical ice crystals, to obtain ice crystal shape information, and to determine ice crystal orientation properties.

2. Polarized Radiative Transfer in Ice Clouds

[5] We shall consider an optically anisotropic medium where the single scattering parameters are dependent on the direction of the incident light beam. In this case, the conventional optical depth (defined in the vertical direction) cannot be used to formulate the transfer of diffuse intensity vector. However, we may define a differential normal optical depth such that $d\tilde{\tau} = \tilde{\beta}_e dz$, where the vertical extinction coefficient $\tilde{\beta}_e = \beta_e(\mu = 1)$, $\mu = \cos\theta$, θ is the zenith angle, and z is the distance. The general equation governing the transfer of the Stokes vector in plane-parallel atmospheres can be expressed in the form

$$\mu \frac{d\mathbf{I}(\tilde{\tau}, \mu, \phi)}{d\tilde{\tau}} = \mathbf{k}(\mu)\mathbf{I}(\tilde{\tau}, \mu, \phi) - \frac{1}{4\pi}\int_0^{2\pi}\int_{-1}^{1} \mathbf{k}(\mu')\,\tilde{\boldsymbol{\omega}}(\mu')\mathbf{Z}(\mu, \phi; \mu', \phi')\mathbf{I}(\tilde{\tau}, \mu', \phi')d\mu' d\phi' - \frac{1}{4\pi}\mathbf{k}(-\mu_0)\tilde{\boldsymbol{\omega}}(-\mu_0)\mathbf{Z}(\mu, \phi; -\mu_0, \phi_0)\mathbf{F}_\odot \exp[-\mathbf{k}(-\mu_0)\tilde{\tau}/\mu_0] - \mathbf{k}(\mu)[1 - \tilde{\boldsymbol{\omega}}(\mu)]B(T)\mathbf{I}_e, \quad (1)$$

where the Stokes vector $\mathbf{I}$ consists of four elements defined by (I, Q, U, V); the actual extinction coefficient normalized by the vertical extinction coefficient $\mathbf{k}(\mu) = \boldsymbol{\beta}_e(\mu)/\tilde{\beta}_e$; the single scattering albedo $\tilde{\boldsymbol{\omega}}(\mu) = \boldsymbol{\beta}_s(\mu)/\boldsymbol{\beta}_e(\mu)$; $\boldsymbol{\beta}_s$ is the scattering coefficient matrix that has a similar form as the extinction coefficient matrix; $\mathbf{F}_\odot$ represents the Stokes vector for the incident solar irradiance; $B(T)$ is the Planck intensity at temperature T; $\mathbf{I}_e = (I, Q_e, 0, 0)$, with $-Q_e$ the linear polarization component associated with emission; and $\mathbf{Z}(\mu, \phi; \mu', \phi')$ is the phase matrix [*Chandrasekhar*, 1950]. In equation (1), the second term on the right-hand side denotes the multiple scattering contribution, while the third and fourth terms represent, respectively, the contributions from direct solar radiation and thermal emission from a medium having a temperature T. For wavelengths shorter than about 3.7 μm, thermal

0094-8276/02/2001GL014613$05.00

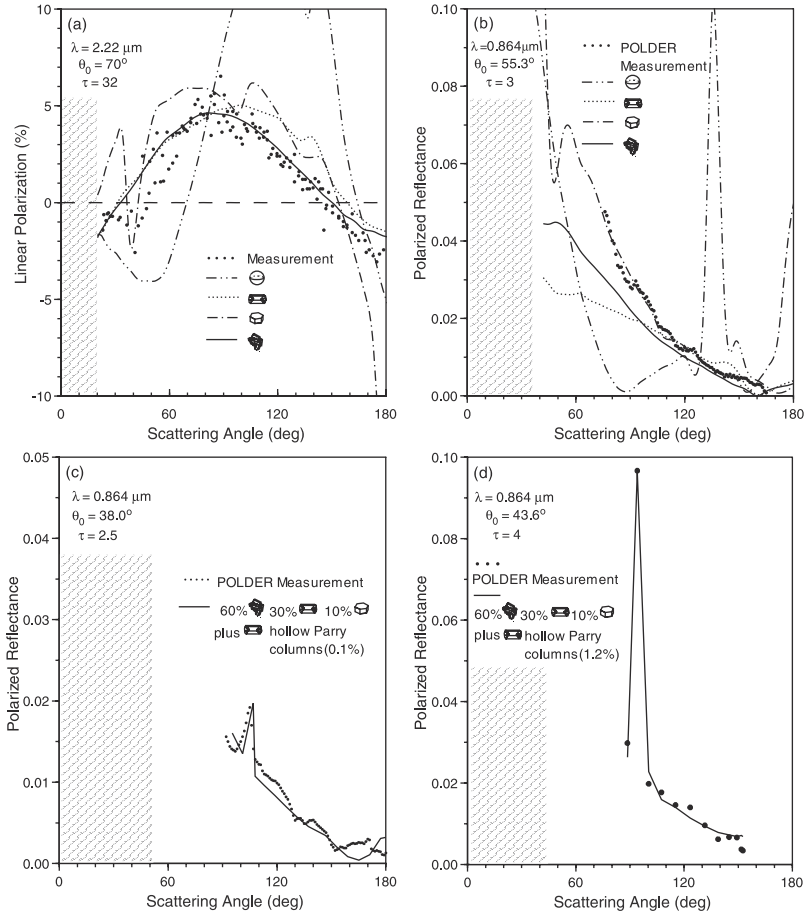

Figure 1. (a) Linear polarization of sunlight reflected from a cirrus cloud measured by an airborne infrared polarimeter at 2.2 μm [*Coffeen*, 1979]. (b) and (c) Full polarization observed from an airborne POLDER instrument at 0.864 μm over an extended cirrus cloud system [*Chepfer et al.*, 1999a]. (d) Same as (b) and (c) but on the ADEOS-1 satellite platform [*Chepfer et al.*, 1999b]. The theoretical results are computed for randomly oriented hollow columns, plates, and irregular aggregates, and ice spheres. In (c) and (d), a small percentage of hollow Parry columns is added to produce the observed peaks. The shaded areas denote scattering angle regions where the reflected sunlight is out of the observation range for the solar zenith angles given in the figures.

emission within the earth-atmosphere system can be neglected in comparison to radiation from the sun. For wavelengths longer than 5 μm, the reverse is true. Between 3.7 and 5 μm, the relative importance of thermal emission and solar reflection for a cloud layer depends largely on the position of the sun and the cloud temperature.

[6] In general, the scattering phase matrix **P** consists of 16 elements and is a function of the incoming (μ', ϕ') and outgoing (μ, ϕ). If the particles are randomly oriented in space and have a plane of symmetry, the scattering phase matrix **P** consists of only six independent elements [*van de Hulst*, 1957]. In this case, $\mathbf{k}(\mu) = 1$ and β_s, β_e, and $\tilde{\omega}$ are independent of μ. For the case of horizontally oriented ice crystals, we found from the analysis of light scattering results that the polarized and cross-polarization components of the extinction coefficients with respect to the incident Stokes vector are negligibly small and that for all practical purposes, we may use the scalar extinction and scattering coefficients in numerical calculations [see also *Mishchenko et al.*, 2002]. Based on numerical analysis, we find that the upper right and lower left four elements in the scattering phase matrix are close to zero so that

$$\mathbf{P} \cong \begin{pmatrix} P_{11} & P_{12} & 0 & 0 \\ P_{21} & P_{22} & 0 & 0 \\ 0 & 0 & P_{33} & P_{34} \\ 0 & 0 & P_{43} & P_{44} \end{pmatrix}, \qquad (2)$$

where P_{11} denotes the normalized phase function, P_{12} represents the degree of linear polarization, and other elements are produced by the cross components of electric fields. These elements can be computed from a unified theory for light scattering by ice crystals innovated by *Liou et al.* [2000]. For ice particles randomly oriented in three-dimensional space, we find $P_{21} = P_{12}$ and $P_{43} = -P_{34}$. In the case of spherical particles, in addition to the preceding conditions, we also have $P_{22} = P_{11}$ and $P_{44} = P_{33}$, and so there are only four elements.

[7] Once the scattering phase matrix is defined, we may approach the radiative transfer problem involving ice particles randomly oriented in a horizontal plane using the adding method [*Takano and Liou*, 1989]. The phase function and single scattering parameters are now dependent on the direction of the incident beam. We may define reflection and transmission functions based on single scattering and optically thin approximations to formulate the adding equations. However, in the case of solar radiation, we must use the normal optical depth $\tilde{\tau}$ and the single scattering albedo, which is dependent on the cosine of the solar zenith angle. We must also distinguish between the reflection and transmission functions for radiation from above and below, since the phase matrix for horizontally oriented ice particles differs in these two configurations. Moreover, in the adding equations, the optical depth is replaced by $\mathbf{k}(-\mu_0)\tilde{\tau}_{a,b}$, where a and b denote the indices for the two layers.

3. Interpretation of Polarization Measurements

[8] Airborne measurements of the reflected intensity and linear polarization of sunlight from clouds have been made by *Coffeen* [1979] using an infrared polarimeter. The near infrared window wavelengths were selected to minimize the polarization contribution from Rayleigh scattering and water vapor absorption. Observations of a few dozen cloud systems were carried out over the Caribbean and western Atlantic. Figure 1a displays an observed linear polarization ($-Q/I$) pattern on the solar principal plane ($\phi - \phi_0 = 0°/180°$) at 2.2 μm from a 5 km thick cirrus cloud when the solar zenith angle was 70°. Also shown are a number of theoretical linear polarization results computed for randomly oriented plates, hollow columns, and irregular aggregates with rough surfaces, as well as ice spheres. In the interpretation, we first determined the cirrus optical depth that best matched the observed data. In this case, we found after numerous theoretical calculations that $\tau = 32$ was the best value. We then selected typical sizes for the three ice crystal shapes. For plates, we used a size with a length (L) to width ($2a$, two times the conventional radius) ratio of 16/80 μm, while a size of 100/40 μm with a hollow depth of 25 μm was selected for columns. The irregular aggregates were constructed from six solid columns with rough surfaces, the maximum length of which was approximately equivalent to the column case. The ice spheres used had a mean effective radius of 81 μm.

[9] The spherical case had a maximum linear polarization of 35% located at about the 127° scattering angle corresponding to the primary rainbow feature, as well as a negative polarization maximum at about 50°. These patterns deviate significantly from the observed data and, thus, cirrus clouds cannot contain spherical ice particles. The results computed for the three nonspherical shapes are close to the observed pattern, with the irregular aggregate case revealing a best general comparison, except in the region from 20° to 50°, in association with the negative polarization produced by 22° and 46° halo patterns, as well as in the backscattering directions from 170° to 180°. The solid plate case produced a negative polarization of about 3% at about 40°, and a significant negative polarization at backscattering, which differed from the linear polarization patterns involving hollow columns and irregular aggregates. We found that a combination of 50% aggregates, 25% columns, and 25% plates not shown in the figure produced the best visual fit to the observed data.

[10] Analysis of the observed polarization patterns from the POLDER instrument has been reported by *Chepfer et al.* [1999a, 1999b]. This instrument consists of a number of wavelengths, three of which, at 0.443, 0.670 and 0.864 μm, were used for polarization measurements. The measured parameter is referred to as the polarized reflectance defined by $\pi(Q^2 + U^2 + V^2)^{1/2}/\mu_0 F_\odot$, where μ_0 is the cosine of the solar zenith angle and $F_\odot$ is the solar irradiance. At infrared wavelengths, reflectance from the earth's surface is not polarized and consequently $Q = U = V = 0$. Thus, the polarized reflectance is independent of the surface albedo. Moreover, at the infrared wavelength of 0.864 μm, the polarized reflectance produced by Rayleigh scattering and the effect of water vapor absorption can also be neglected. The optical depth due to Rayleigh scattering at 0.864 μm is 0.016, which can be accounted for in the interpretation of optical depth. The measured polarized reflectance data shown in Figure 1b is taken from *Chepfer et al.* [1999a] in which the solar zenith angle is 55.3°. These data were collected from an aircraft over an extended cirrus cloud system off the coast of Brittany, France, on 17 April, 1994. The optical depth for various types of ice particles that best fits the data is $\tau = 3$. Again, the ice sphere case produced a large maximum polarization pattern at about 136°, which is not contained in the observed data. For the three ice crystal shapes, we found that the results computed for randomly oriented thin plates with a size of $L/2a$ of 8/80 μm matched the observed data most closely, except in the 160°–180° backscattering directions. In this scattering region, the patterns of randomly oriented hollow columns and irregular aggregates showed close comparisons, except at the scattering angle of 160°. Because the polarization values in this scattering angle region are so small, it is not clear whether there was a problem in the data reduction from POLDER measurements. Based on these comparisons, it appears appropriate to conclude that the top of the extended cirrus in this case consists of a majority of randomly oriented thin plates with a half width (radius) of about 40 μm.

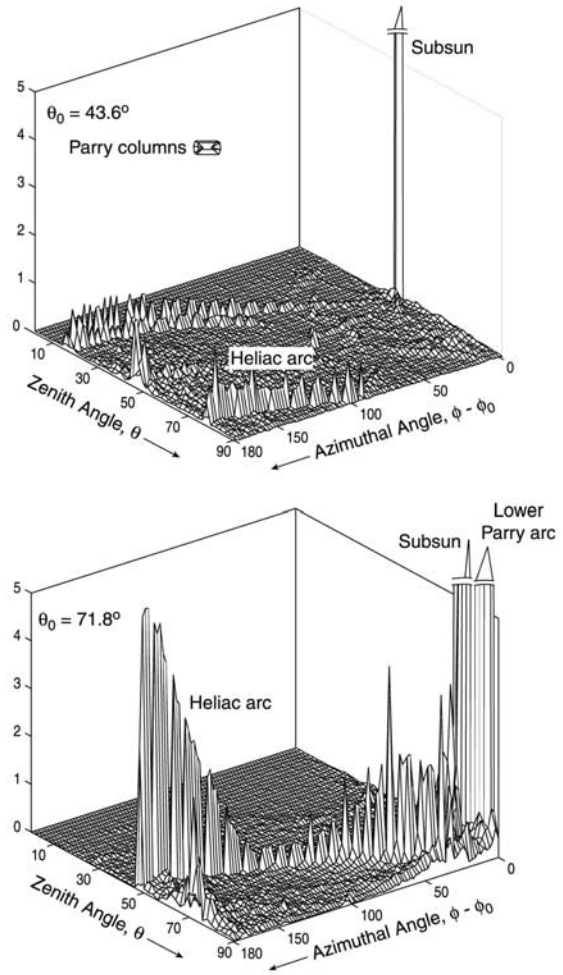

Figure 2. Three-dimensional phase function P_{11} as a function of zenith and azimuthal angles for hollow Parry columns for solar zenith angles of (a) 43.6° and (b) 71.8° at 0.864 μm. For (a), a subsun peak feature is shown on the solar principal plane ($\phi - \phi_0 = 0°$) along with weak heliac arc features. For (b), because of the lower sun elevation angle, an additional lower Parry arc is produced along with stronger heliac arc features.

[11] Figures 1c and 1d display POLDER measurements from cirrus clouds containing some horizontally oriented ice crystals. The polarized reflectance results in Figure 1c are taken from the aforementioned cirrus cloud case (Figure 1b), but with a solar zenith angle of 38.0°. The data displayed in Figure 1d corresponds to a cirrus at a time between October 1996 and June 1997 determined from the POLDER on board the ADEOS-1 satellite platform [*Chepfer et al.*, 1999b]. There are distinct peaks located at about 105° and 94° scattering angles in Figures 1c and 1d, respectively. These peaks cannot be produced by the results computed from randomly oriented ice crystals presented above. Again, we first found the optical depths that best

matched the observed data, which were $\tau = 2.5$ and 4, respectively. Subsequently, we used the individual results for irregular aggregates, hollow columns, and plates to compare with the data points, and found that a combination of 60%, 30%, and 10%, respectively, matched the observed data without the peak features most closely. To match these peaks, we had to add 0.1% and 1.2% horizontally oriented hollow columns, referred to as hollow Parry columns, as shown in Figures 1c and 1d, respectively. The interpretation of polarization measurements from ice crystal clouds is obviously nonunique and the results presented in these two figures are but two combinations that produced the best matches. Nevertheless, these comparisons reveal that the two cirrus clouds under polarization observation contained nonspherical ice crystals with a majority of irregular aggregates averaged in the vertical direction and that a small fraction of hollow Parry columns must have existed in these clouds. Although the computer time involved in the preceding calculations was moderate, to establish an automated retrieval algorithm for the determination of the shape, size, and orientation of ice particles based on polarization technique requires further in-depth research and development.

[12] To understand the peak features measured from the reflected polarization of sunlight, we present in Figure 2 the scattering phase function P_{11} for hollow Parry columns in the plane below the horizon for two incident solar zenith angles: 43.6°, corresponding to the POLDER measurements discussed above, and 71.8°, for illustration purposes. In the former, the peak located at the solar principal plane ($\phi - \phi_0 = 0°$) and the zenith angle of about 44° is the subsun feature, produced by the external reflection of light beams from the flat column surface. The peaks displayed in Figures 1c and 1d are associated with this subsun feature. Because of the horizontal orientation of column crystals, reflected light beams combine in certain directions, notably the heliac arc is associated with an external reflection involving a sloping prism face. More impressive features are generated for a larger solar zenith angle of 71.8°, i.e., the solar elevation angle of 19.2°. In addition to the subsun feature and the heliac arc, a lower Parry arc associated with the 22° halo can also be produced from the light beams undergoing two refractions. Finally, it should be noted that the phase functions for randomly oriented plates, hollow columns, irregular aggregates, and other ice crystal shapes can be found in our recent paper [*Liou et al.*, 2000].

4. Concluding Remarks

[13] We have developed a theoretical framework for the computation of polarized radiative transfer in cirrus clouds containing randomly and horizontally oriented ice crystals. In the case involving horizontal orientation, the phase matrix corresponding to the Stokes vector consists of 16 nonzero elements in principle and its dependence on directionality cannot be expressed in terms of the scattering angle but must be defined by the incoming and outgoing directions. The physical meanings of optical depth must also be redefined to account for its dependence on the incoming light beam.

[14] We have demonstrated that polarization of sunlight reflected from clouds can be employed to identify the shape of cloud particles. The polarization patterns located at the well-known rainbow features in the backscattering direction at about 125°–140° can be used to discriminate spherical water droplets (water clouds) and nonspherical ice crystals (ice clouds). Second, we showed that in the case of ice clouds, the ice crystal size and shape can be inferred from linear or full polarization patterns. From the limited polarization observations that were available, we found that a combination of various ice crystal shapes produced the best interpretation. Finally, we illustrated that the reflected polarization from ice clouds contains peak features that can only be produced by horizontally oriented ice columns/plates. Reflected polarization thus provides a means to infer the orientation of nonspherical ice crystals, information that cannot be obtained globally from other remote sensing techniques.

[15] **Acknowledgments.** This research was supported by National Science Foundation Grant ATM-99-07924, NASA Grant NAG5-7738, and DOE Grant DE-FG03-00ER62904. We thank Dr. Helene Chepfer for making available to us the data published in her papers.

References

Chandrasekhar, S., *Radiative Transfer*, Oxford Univ. Press, Oxford, 1950.

Chepfer, H., G. Brogniez, L. Sauvage, P. H. Flamant, V. Trouillet, and J. Pelon, Remote sensing of cirrus radiative parameters during EUCREX'94. Case study of 17 April 1994. Part II: Microphysical models, *Mon. Wea. Rev.*, *127*, 504–519, 1999a.

Chepfer, H., G. Brogniez, P. Goloub, F. M. Brèon, and P. H. Flamant, Observations of horizontally oriented ice crystals in cirrus clouds with POLDER-1/ADEOS-1, *J. Quant. Spectrosc. Radiat. Transfer*, *63*, 521–543, 1999b.

Coffeen, D. L., Polarization and scattering characteristics in the atmosphere of Earth, Venus, and Jupiter, *J. Opt. Soc. Am.*, *69*, 1051–1064, 1979.

Hansen, J. E., and J. W. Hovenier, Interpretation of the polarization of Venus, *J. Atmos. Sci.*, *31*, 1137–1160, 1974.

Liou, K. N., and Y. Takano, Light scattering by nonspherical particles: Remote sensing and climate implications, *Atmos. Res.*, *31*, 271–298, 1994.

Liou, K. N., Y. Takano, and P. Yang, Light scattering and Radiative transfer in ice crystal clouds: Application to climate research, in *Light Scattering by Nonspherical Particles*, edited by M. I. Mishchenko, J. Hovenier, and L. D. Travis, Academic Press, San Diego, 2000.

Lyot, B., Recherches sur la polarization de la lumière des planètes et de quelques substances terrestres, *Ann. Observ. Paris (Meudon)*, *8*, 161 pp., 1929, [available in English as NASA TTF-187, 1964].

Mishchenko, M. I., L. D. Travis, and A. A. Lacis, *Scattering, Absorption, and Emission of Light by Small Particles*, Cambridge Univ. Press, Cambridge, 2002.

Takano, Y., and K. N. Liou, Solar radiative transfer in cirrus clouds. Part II: Theory and computation of multiple scattering in an anisotropic medium, *J. Atmos. Sci.*, *46*, 20–36, 1989.

Takano, Y., and K. N. Liou, Transfer of polarized infrared radiation in optically anisotropic media: Application to horizontally oriented crystals, *J. Opt. Soc. Amer. A*, *10*, 1243–1256, 1993.

van de Hulst, H. C., *Light Scattering by Small Particles*, Wiley, New York, 1957.

K. N. Liou and Y. Takano, Department of Atmospheric Sciences, University of California, Los Angeles, 405 Hilgard Ave., Los Angeles, CA 90095-1565, USA. (knliou@atmos.ucla.edu)